

Design and Performance Evaluation of Solar Gas Turbine Power Plant in South Western Algeria

Imad Eddine Meriche*[‡], Abdelhadi Baghidja*, Taqiy Eddine Boukelia*

*Department of Mechanics, University of Constantine1, Laboratory of Renewable Energies and Durable Development, Algeria
(imad-113@live.fr, abeghidja1@yahoo.fr, taqy25000@hotmail.com)

[‡] Corresponding Author; Imad Eddine Meriche, 58 Street Aben Badis –Jijel, Algeria, +213 0791294126, , imad-113@live.fr

Received: 14.01.2014 Accepted: 09.03.2014

Abstract- Hybrid solar tower power plants which use high concentration optics and high temperature air receivers are one of the most important candidates to provide a major share of the clean and renewable energy needed in the future. Computer model and simulation capability are developed in this study to evaluate the performance of a new solar tower power plant with a capacity of 20.5 MWe. The numerical simulation of gas turbine, solar field and tower receiver was performed by using a FORTRAN code based on ray tracing technique (Monte Carlo) and TRNSYS 16 software including TEES and STEC.03 libraries. All thermodynamic parameters of the installation such as pressure ratio, air flow, fuel consumption and concentrated solar power introduced are discussed. This study has for main objective to calculate the energetic and exergetic efficiencies of hybrid and solar electric cycles for two operating systems of the installation, first without regenerator then with regenerator and evaluate their feasibility in the south-western Algerian area.

Keywords Solar Tower, Volumetric Receiver, Gas Turbine, Regenerator, Energetic and Exergetic Analysis

1. Introduction

With the rising price of fossil fuels, renewable energies have the potential to provide the world a clean and cost competitive power in the future. Nowadays, solar power plants are one of the important candidates to provide a major share of the clean electrical energy [1]. There are currently two approaches for generating electricity from solar energy, conversion of solar radiation directly into electricity (photovoltaic panels) and concentrating solar power systems technologies (CSP), this concept is based on concentrating and focusing the direct solar irradiation with mirrors onto receivers' surfaces, this transfers the thermal energy into conventional power cycles using steam turbines, gas turbines or sterling engines [2].

Solar tower power plants are in the class of solar central receiver systems, which use many sun tracking mirrors called heliostats to concentrate and reflect the incident sunlight onto a receiver atop of a tower; the absorbed solar energy is translated into thermal power to generate electricity by Rankin cycle or Brayton cycle [2, 3].

In a solar gas turbine tower, the absorbed solar energy is used to heat the pressurized air before entering the

combustion chamber of the gas turbine, the high temperature of the air is used to drive a Brayton power cycle [3], figure 1.

The first solar hybrid gas turbine system has been tested in the SOLGATE project, using a modified 260 kW (cycle of helicopter turbine) installed at the CESA-1 with the volumetric receiver system at PSA in Spain [4]. A similar scheme of SOTGATE project has been tested in Themis (France), with a 1.4 MWe recuperative gas turbine [5], Schwarzbozl et al [6] design and validate three solar gas turbine systems, Heron H1 (air intercooler) with ISO (international standard organization) rating 1.4 MWe, Solar Mercury 50 (recuperated single shaft engine) with ISO rating 4.2 MWe and PGT 10 simple gas turbine with ISO rating 11.1 MWe and 16.1 MWe with combined cycle.

The first modular volumetric receiver with an outlet temperature up to 960 °C was tested by Heller et al [7] at REFOS project.

In contribution of solar gas turbine modelling research, the present work asks a numerical study and simulation development of high output solar tower power plant based on a hybrid cycle with closed volumetric receiver.

In this work we add a regenerator as an additional component which will recover the latent heat of fume exhausted and used to preheat the pressurized air downstream from the solar receiver, figure 2.

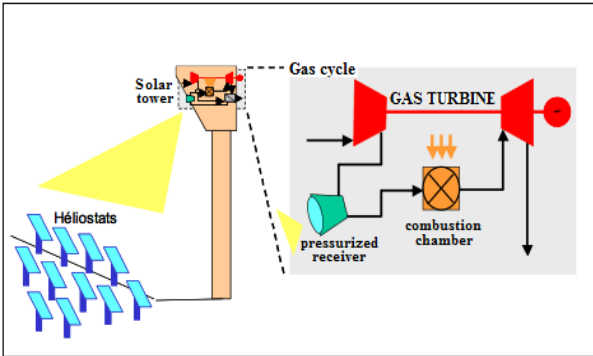


Fig. 1. Solar tower power plant with Brayton cycle [5]

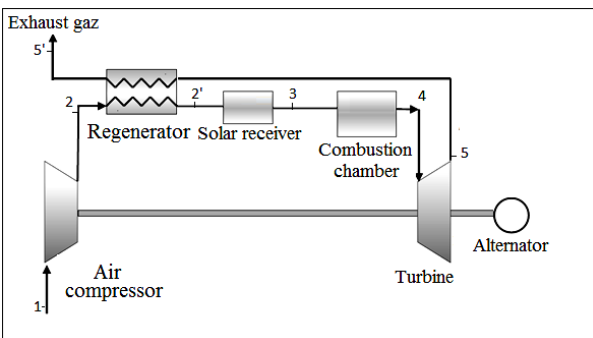


Fig. 2. Physical model of installation with regeneration

2. Potential Solar Energy in Algeria

To design and operate any solar power plants, it is required to have a good meteorological condition data on the site, by including high direct radiation, suitable water supply, flat topography, access to electric transmission facilities and availability of auxiliary fuel supplies [4].

Algeria is one of the countries enjoying an enormous potential of solar energy, it is located between latitudes 19°N and 37°N, longitudes 9°W and 12°E with a land area equal to 2.381.741Km² and over 70% of this area consists of deserts [8]. The climatic conditions in southern Algeria are characterized by abundant sunshine throughout the year, low precipitation and humidity, and plenty of unused flat areas especially in the Sahara region (1.787.000 Km²), according to the study of the German aerospace centre, Algeria possesses the largest long term land potential for concentrating solar thermal power plants (CSP) [9,10]. According to the irradiation maps, the annual direct normal irradiation ranges between 2000 kWh/m²/Yr to over 2700 kWh/m²/Yr, and it is accounted among the best sunny areas in the world [11].

In the present study, the chosen site is the region of Béchar (Latitude 31.61°N and Longitude -2.23°E) figure 3, [12].



Fig. 3. Geographic location of Béchar

3. Mathematical Formulation

3.1 Energy Balance

3.1.1 Air Compressor

The air compressor input power is found at:

$$\dot{W}_C = \dot{m}_a C p_a (T_2 - T_1) \tag{1}$$

$$\text{And : } T_2 = T_1 \left(1 + \frac{1}{\eta_{AC}} \left(r_{AC}^{\frac{\gamma_a - 1}{\gamma_a}} - 1 \right) \right) \tag{2}$$

$$C p_a (T) = 1.048 - \left(\frac{3.83 T}{10^4} \right) + \left(\frac{9.45 T^2}{10^7} \right) - \left(\frac{5.49 T^3}{10^{10}} \right) + \left(\frac{7.92 T^4}{10^{14}} \right) \tag{3}$$

3.1.2 Volumetric Receiver

The thermal power exchanged between the interior of receiver cavity and pressurized air is:

$$\dot{Q}_{ex} = \dot{m}_{air} C p (T_3 - T_2') = \dot{Q}_r \tag{4}$$

The field matrix of solar effectiveness [13, 14, 15] includes the reflectivity of the mirror (ρ_{MIRR}), the effect cosine (η_{cos}), the effect shades and blockings ($\eta_{Block,shad}$), the effect atmospheric (η_{Atmos}), and the interception effect (η_{Int}), figure 4.

$$\eta_{field} = \rho_{MIRR} \times \eta_{cos} \times \eta_{Block,shad} \times \eta_{Atmos} \times \eta_{Int} \tag{5}$$

With:

$$\eta_{cos} = \frac{\sqrt{2}}{2} [\sin(\alpha) \cos(\lambda) - \cos(\theta_H - A) \cos(\alpha) \sin(\lambda) + 1]^{0.5} \tag{5.1}$$

$$\eta_{Atmos} = \begin{cases} 0.99321 - 0.000176 S_0 + 1.97 \cdot 10^{-8} S_0^2 ; S_0 \leq 1000m \\ \exp(-0.0001106 S_0) ; S_0 > 1000m \end{cases} \tag{5.2}$$

$$\eta_{intercept} = \frac{1}{2\pi \sigma_{tot}^2} \int(x) \int(y) \exp\left(\frac{-x^2+y^2}{2 \sigma_{tot}^2}\right) dx dy \tag{5.3}$$

$$\sigma_{tot} = (\sigma_{solaire}^2 + \sigma_{miroir}^2 + (2 \sigma_{track})^2)^{0.5} \quad (5.4)$$

$\eta_{Block,shad}$: The value is obtained by positioning of the heliostats field (HFLD code) [16].

The thermal power received by the sensor surface of heliostats (S_c) in the cavity of receiver is written:

$$\dot{Q}_c = \eta_{field} I_c S_c \quad (6)$$

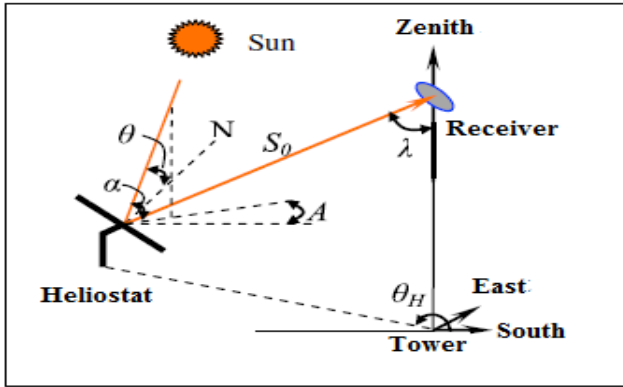


Fig. 4. Position and angles of the heliostat relative to the receiver [14]

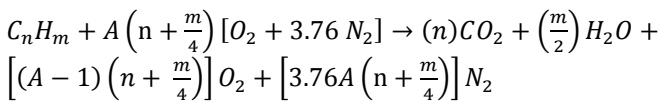
The cavity of the volumetric receiver loses a fraction of this power per reflection, convection natural and radiation [17, 18], the power transmitted (\dot{Q}_r) by the cavity of the receiver is:

$$\dot{Q}_r = \dot{Q}_c - h_{cv} A_r (T_r - T_0) - \sigma \epsilon A_r (T_r^4 - T_0^4) \quad (7)$$

A_r : Receiver area, h_{cv} : Coefficient of convection transfer.
 σ : Stefan Boltzmann constant ($5,670 \times 10^{-8} \text{W/m}^2 \cdot \text{K}^4$)
 ϵ : Absorber emissivity.

3.1.3. Combustion Chamber

In the combustion chamber, the natural gas is injected and burned with the pressurized air



$$\dot{m}_a h_3 + \dot{m}_f \text{LHV} = \dot{m}_g h_4 + (1 - \eta_{cc}) \dot{m}_f \text{LHV} \quad (8)$$

3.1.4. Turbine

The gas turbine output power is also found as:

$$\dot{W}_T = \dot{m}_g C p_g (T_4 - T_5) \quad (9)$$

$$T_5 = T_4 \left(1 - \eta_T \left(1 - \left(\frac{P_4}{P_5} \right)^{\frac{1-\gamma_g}{\gamma_g}} \right) \right) \quad (10)$$

3.1.5. Regenerator

Regenerator uses the turbine exhaust gases to preheat the compressed air before entering into the combustion chamber:

$$\text{Eff} = \frac{(T_2' - T_2)}{(T_5 - T_5')} \quad (11)$$

3.1.6. Alternator

The electric output power is also found as:

$$P_{ele} = W_{GT} \cdot \eta_{al} \quad (12)$$

3.1.7. Exergy Balance

Exergy is divided into two components: physical and chemical [19]. The physical exergy is defined as the theoretical maximum useful work of a system that acts to another with a reference environment and a state of equilibrium. The chemical exergy is associated with the chemical composition on the system and the chemical composition of the reference environment.

Applying the second law of thermodynamics, an exergy balance can be obtained:

$$\dot{E}x_Q + \sum_i \dot{m}_i ex_i = \sum_e \dot{m}_e ex_e + \dot{E}x_W + \dot{E}x_D \quad (13)$$

$$\dot{E}x_Q = \left(1 - \frac{T_0}{T_i} \right) \dot{Q}_i \quad (14)$$

$$\dot{E}x_W = \dot{W} \quad (15)$$

$$ex = ex_{ph} + ex_{ch}^{mix} \quad (16)$$

$$ex_{ph} = (h - h_0) - T_0 (s - s_0) \quad (17)$$

$$ex_{ch}^{mix} = \left[\sum_{i=1}^n x_i ex_{ch}^{i} + RT_0 \sum_{i=1}^n x_i \ln x_i \right] \quad (18)$$

$\dot{E}x_Q, \dot{E}x_W$: Thermal exergy and power exergy .

ex_{ph}, ex_{ch} : Physical exergy and chemical exergy of the gas mixture

3.2.1. Heliostat Fields

Exergy expression of the heliostats fields is given as:

$$Ex_{hel} = Ex_{rec} + Ex_{hel,lous} \quad (19)$$

Exergy efficacy of the heliostats fields is:

$$\eta_{ex, hel} = \frac{Ex_{rec}}{Ex_{hel}} \quad (20)$$

3.2.2. Volumetric Receiver

Exergy expression of the solar receiver [20] is given as:

$$Ex_{rec} = Ex_{rec,abs} + Ex_{rec,lous} + IR_{rec} \quad (21)$$

$Ex_{rec,abs}, Ex_{rec,lous}$ is Exergy absorbed by the receiver and Exergy loused by the receiver and IR_{rec} is the irreversibility of solar receiver.

The exergy efficacy of the solar receiver is:

$$\eta_{ex, rec} = \frac{Ex_{rec,abs}}{Ex_{rec}} \quad (22)$$

3.2.3. Brayton Cycle

Expression of exergetic efficiencies of the various components of the gas turbine are in table 1 [21].

Table 1. Exergetic efficiencies of the gas turbine

Component	Exergy destruction	Exergy Efficiency
Compressor	$\dot{E}x_{D,AC} = \dot{E}x_1 - \dot{E}x_2 + \dot{W}_{AC}$	$\eta_{ex,Comp} = \frac{\dot{E}x_2 - \dot{E}x_1}{\dot{W}_{AC}}$
Combustion chamber	$\dot{E}x_{D,CC} = \dot{E}x_3 + \dot{E}x_f - \dot{E}x_4$	$\eta_{ex,CC} = \frac{\dot{E}x_4}{\dot{E}x_3 + \dot{E}x_f}$
Turbine	$\dot{E}x_{D,GT} = \dot{E}x_4 - \dot{E}x_5 - \dot{W}_{GT}$	$\eta_{ex,Tur} = \frac{\dot{W}_{GT}}{\dot{E}x_4 - \dot{E}x_5}$
Regenerator	$\dot{E}x_{RG} = \dot{E}x_{IN} - \dot{E}x_{OUT}$	$\eta_{ex,RG} = \frac{\dot{E}x_{2'} - \dot{E}x_2}{\dot{E}x_5 - \dot{E}x_{5'}}$

4. Simulation and Parameters of the Installation

To calculate the radiation view factor we use an algorithm which develops a Monte-Carlo method (tracing technique), this technique calculates a vector leaving the originating surface at a random location, angle and elevation, and checks if it intersects the polygon on the target surface [18,22]. The Monte-Carlo ray tracing technique was applied and coded into FORTRAN language; the code is validated by the SOLTRACE simulator [5] and inserted in TRNSYS model (the TRNSYS software database is coded in Fortran, for that the code set is coded in Fortran).

The design of the optics and the thermal models part of the solar gas turbine tower can be optimized using TRNSYS 16 and STEC 3.0 library (Solar Thermal Electric Components) and TEES library [23], the inputs of the simulation are hourly solar irradiance, meteorological data, ambient temperature, site information and technical system data (heliostats, tower) [24], figure 5.

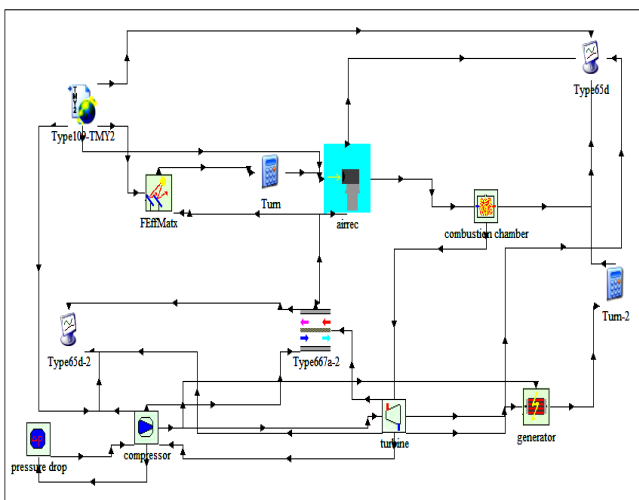


Fig. 5. Simulation of installation in TRNSYS16

4.1. Solar Gas Turbine Model

For the dimension and the operational component parameters of the gas turbine we chose the GE MS5001R gas turbine model (20.5 MWe) [25], the gas turbine and solar tower [4] parameters are given in table 2.

The models parameter and information included heliostats area, solar tower, electric power, heat rate, exhaust mass flow temperature and pressures are implemented and simulated by TRNSYS 16.

Table 2. Designs parameters of installation

Parameters	Valour
Output temperature of combustion chamber	957 °C
Lower calorific value of natural gas (LHV)	45119 kJ/kg
Compressor pressure	10.5 bar
Compressor isentropic efficiency	84 %
Atmospheric conditions	1.132 bars 25°C
Turbine isentropic efficiency	87 %
Chamber combustion efficiency	95 %
Electromechanical efficiency of generator	98 %
Less pressure in the combustion chamber admission air loss pressure	1 %
Air mass flow used in ISO conditions (ṁ)	348000 Kg/hr
Pressure of exhaust fumes	101.5 KPa
Average direct normal irradiation (I)	800 W/m ²
Reflectivity of mirrors	89.23 %
Total error (σ _{tot})	4 mrad
Heliostat reflective area	11×11 m ²
Number of heliostats	900
Receiver area	76.2 m ²
Declination of the receiver aperture	25 Degree

5. The Performance Results of the Installation

5.1. Performance of the Air Compressor

For the parameters of admission (P₀= 1.0135 bars, T₀=25 C°) and a compression up to P₁= 10.5 bars, we obtained by simulating the useful power consumed by the compressor and the temperature of the pressurized air output the compressor, the results are represented in figure 6.

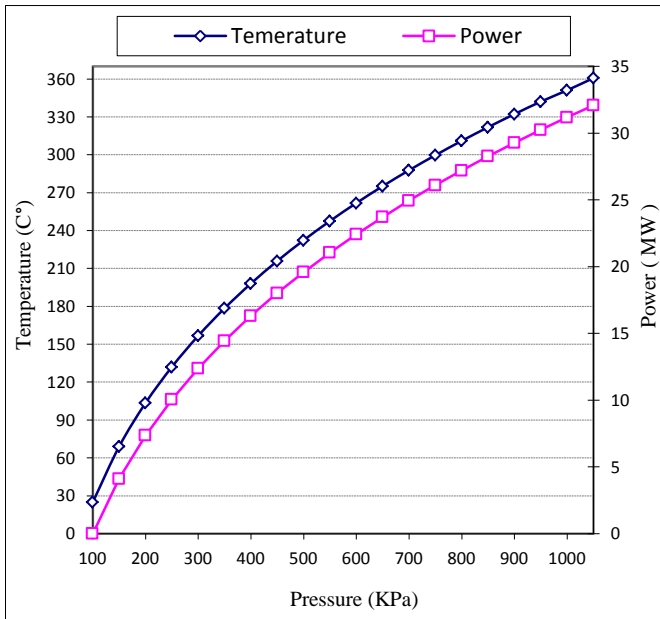


Fig. 6. Variation of the temperature and the compressor power as a function of the rate compression

5.2. Performance of the Solar Collector

With temperature $T_2 = 355.2 \text{ }^\circ\text{C}$ and $P_2 = 10.45 \text{ bars}$ at the entry of the solar receiver, we calculate the received solar energy necessary to obtain a maximum output temperature ($T_3 \text{ max} = 900^\circ\text{C}$), as represented in figure 7.

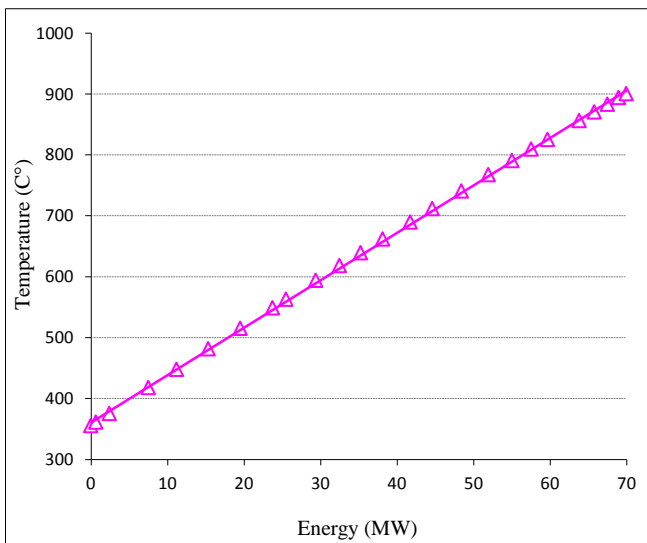


Fig. 7. Variation of air temperature output receiver as a function of the received solar energy

5.3. Influence of the Absorbed Solar Energy in the Installation

Solar receiver output air temperature T_3 has a direct influence on the consumption of natural gas in the combustion chamber, figure 8.

The increase in the output air temperature of solar receiver has a direct impact on the mass flow rate and the useful energy produced, figure 9.

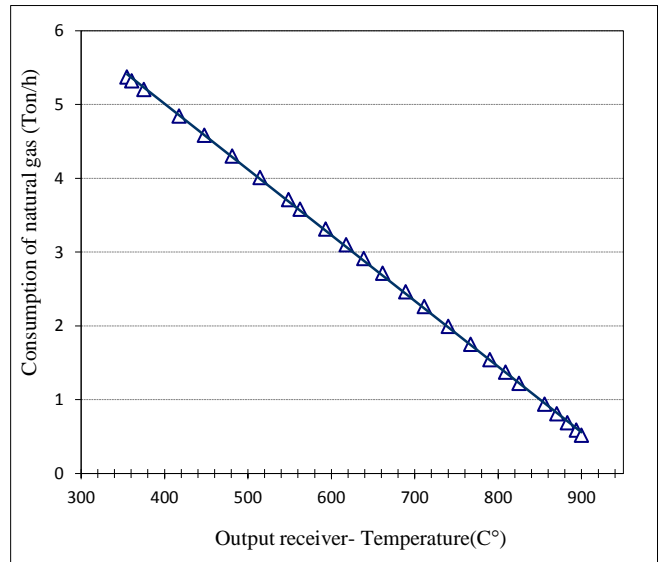


Fig. 8. Consumption of natural gas as a function of temperature air output solar receiver

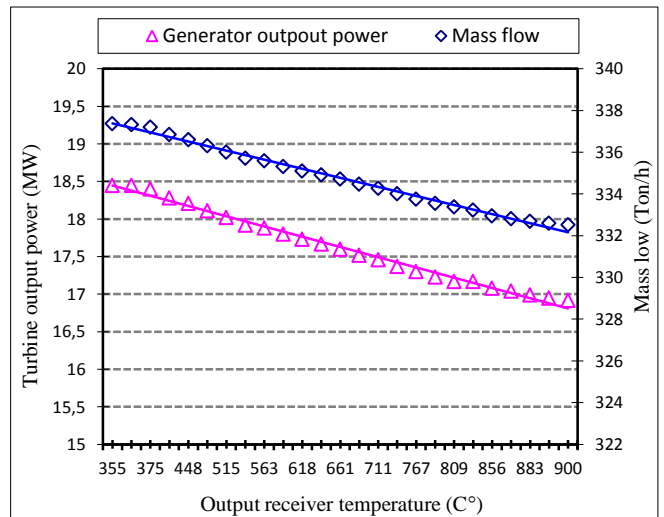


Fig. 9. Variation of mass flow and output power generator as a function of output receiver air temperature

6. Installation Performance Without and With Regeneration

6.1. Performance of Installation Without Regeneration

In the installation without regenerator, the maximum output air temperature of the receiver is limited to 900°C , and outlet air temperature of the combustion chamber to 957°C .

With optimal conditions of the incident solar irradiation and climatic condition of Béchar area, we calculate the solar field efficiencies of the installation.

The efficiencies of the solar field calculated by FORTRAN code and verified by the software SolTrace are given in Table 3.

Table 3. Solar field efficiencies

ρ_{Miroir} %	η_{cos} %	$\eta_{\text{Blocages,Ombres}}$ %	η_{Atmos} %	$\eta_{\text{intercept}}$ %
89.23	89.60	94.45	96.32	99.47

After calculating the solar field efficiencies, we proceed to calculate the energetic and exergetic efficiencies of the installation without regeneration, that for operating conditions ($T_0 = 25 \text{ }^\circ\text{C}$ and $T_{3\text{max}} = 900 \text{ }^\circ\text{C}$), results are displayed in table 4 and table 5.

Table 4. Energy efficiencies of the installations without regeneration

Subset	Energy (MW)	Temperature ($^\circ\text{C}$)	Efficiency (%)
Heliostat field	$P_{\text{hel}} = 96.64$ $Q_C = 69.92$	$T_{\text{amb}} = 25$	$\eta_C = 72.35$
Receiver	$\dot{Q}_C = 69.92$ $\dot{Q}_r = 55.36$	$T_2 = 360$ $T_3 = 900$	$\eta_{\text{rec}} = 79.17$
Gas turbine	$P_{\text{fuel}} = 6.58$ $\dot{W}_{GT} = 17.52$	$T_4 = 957$ $T_5 = 486.5$	-
Solar-electric Cycle	$P_{\text{hel}} = 96.64$ $P_{\text{elec}} = 17$	-	$\eta_{\text{sol-}\acute{e}\text{le}} = 17.59$
Hybrid cycle	$P_{\text{hybrid}} = 61.94$ $P_{\text{elec}} = 17$	-	$\eta_{\text{hyb}} = 27.44$

Table 5. Exergy efficiencies of the installations without regeneration

Subset	Exergy (MW)	Efficiency (%)
Heliostat field	$Ex_{\text{hel}} = 91.64$ $Ex_{\text{rec}} = 66.30$	$\eta_{\text{ex, hel}} = 72.35$
Receiver	$Ex_{\text{rec}} = 66.30$ $Ex_{\text{rec, abs}} = 39.80$	$\eta_{\text{ex, rec}} = 60.03$
Gas turbine	$\dot{E}x_1 - \dot{E}x_2 = 30.08$ $\dot{E}x_4 - \dot{E}x_5 = 46.91$	$\eta_{\text{ex Comp}} = 93.74$ $\eta_{\text{ex CC}} = 75.23$ $\eta_{\text{ex Turb}} = 94.56$
Solar-electric Cycle	$Ex_{\text{hel}} = 91.64$ $Ex_{\text{elec}} = 17$	$\eta_{\text{ex, sys}} = 18.55$

6.2. Performance of Installation With Regeneration

In the installation with the regenerator, the optimal efficiency of the regenerator is around 83% [24]; we calculate the absorbed solar energy corresponding to an output air temperature of the receiver limited at 900°C .

The results of energetic and exergetic efficiencies of the installation with regeneration for operating conditions ($T_0 = 25 \text{ }^\circ\text{C}$ and $T_{3\text{max}} = 900 \text{ }^\circ\text{C}$) are displayed in table 6 and table 7.

Table 6. Energy Efficiencies of the installations with regeneration

Subset	Energy (MW)	Temperature ($^\circ\text{C}$)	Efficiency (%)
Heliostat field	$P_{\text{hel}} = 78.59$ $Q_C = 56.86$	$T_{\text{amb}} = 25$	$\eta_C = 72.35$
Receiver	$\dot{Q}_C = 56.86$ $\dot{Q}_r = 45.05$	$T_{2r} = 478.33$ $T_3 = 900$	$\eta_r = 79.24$
Gas turbine	$P_{\text{fuel}} = 6.58$ $\dot{W}_{GT} = 17.52$	$T_4 = 957$ $T_{5r} = 370.66$	-
Solar-electric Cycle	$P_{\text{hel}} = 78.59$ $P_{\text{elec}} = 17$	-	$\eta_{\text{sol-}\acute{e}\text{le}} = 21.63$
Hybrid cycle	$P_{\text{hybrid}} = 51.63$ $P_{\text{elec}} = 17$	-	$\eta_{\text{hyb}} = 32.92$

Table 7. Exergy efficiencies of the installations with regeneration

Subset	Exergy (MW)	Efficiency (%)
Heliostat field	$Ex_{\text{hel}} = 74.52$ $Ex_{\text{rec}} = 53.91$	$\eta_{\text{ex, hel}} = 72.35$
Receiver	$Ex_{\text{rec}} = 53.91$ $Ex_{\text{rec, abs}} = 33.03$	$\eta_{\text{ex, rec}} = 61.27$
Gas turbine	$\dot{E}x_1 - \dot{E}x_2 = 30.08$ $\dot{E}x_4 - \dot{E}x_5 = 46.81$	$\eta_{\text{ex Comp}} = 93.74$ $\eta_{\text{ex RG}} = 94.15$ $\eta_{\text{ex CC}} = 75.23$ $\eta_{\text{ex Turb}} = 94.56$
Solar-electric Cycle	$Ex_{\text{hel}} = 74.52$ $Ex_{\text{elec}} = 17$	$\eta_{\text{ex, sys}} = 22.81$

6.1 Daily Performances of Installations

To calculate electrical power production and energetic performances of the both installations (without and with regeneration), we take measured values of the incident solar irradiation and climatic condition for two days 22/06/2006 and 21/12/2006 in Béchar area, these dates are chosen in order to avoid under sizing of the heliostats field area [12], figure 10 and figure 11.

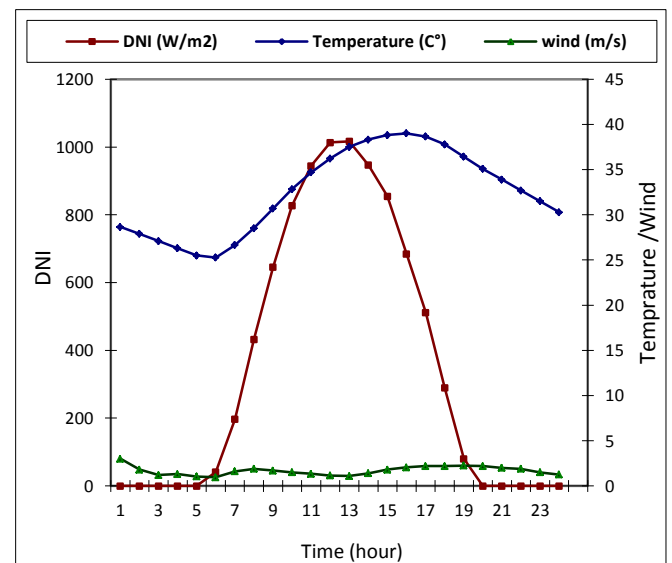


Fig. 10. Daily variation of solar irradiation, temperature and wind in Béchar(22/06/2006)

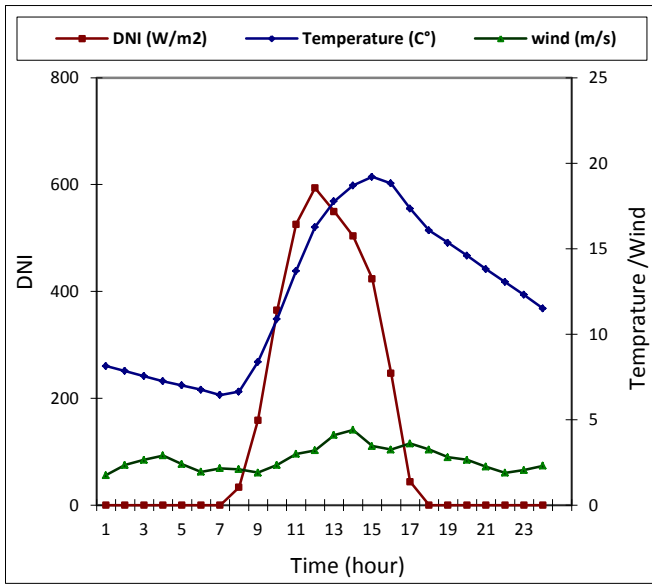


Fig. 11. Daily variation of solar irradiation, temperature and wind in Béchar (21/12/2006)

With the daily variation in figure 10, we calculate the temporal evolution of the powers in both installations, without and with regeneration; results are flowing in figure 12 and figure 13.

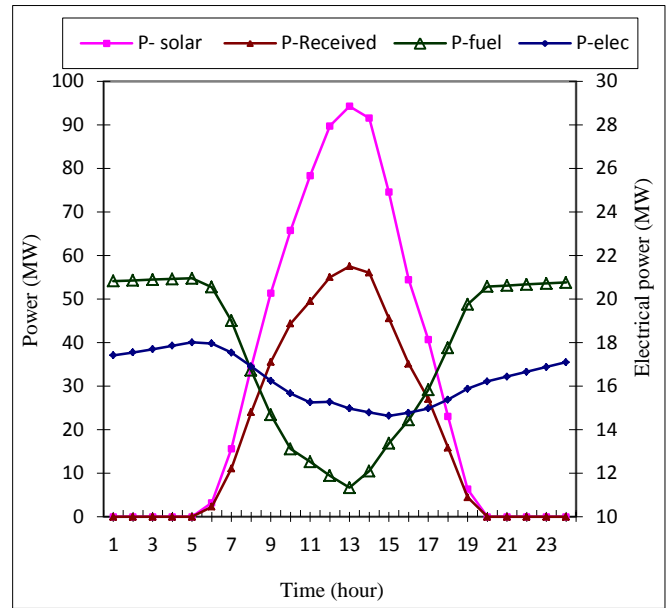


Fig. 13. Temporal evolution of powers in the installation with regeneration (22/06/2006)

With the daily variation in figure 11, we calculate the temporal evolution of the powers in both installations, without and with regeneration; results are flowing in figure 14 and figure 15.

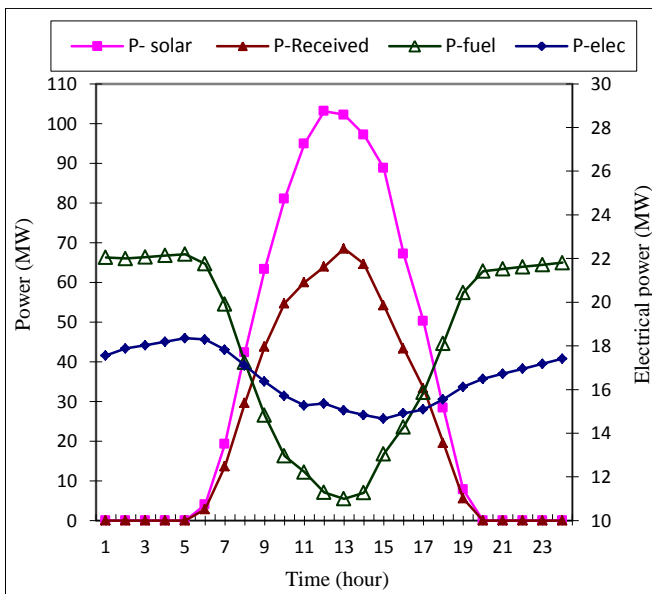


Fig. 12. Temporal evolution of powers in the installation without regeneration (22/06/2006)

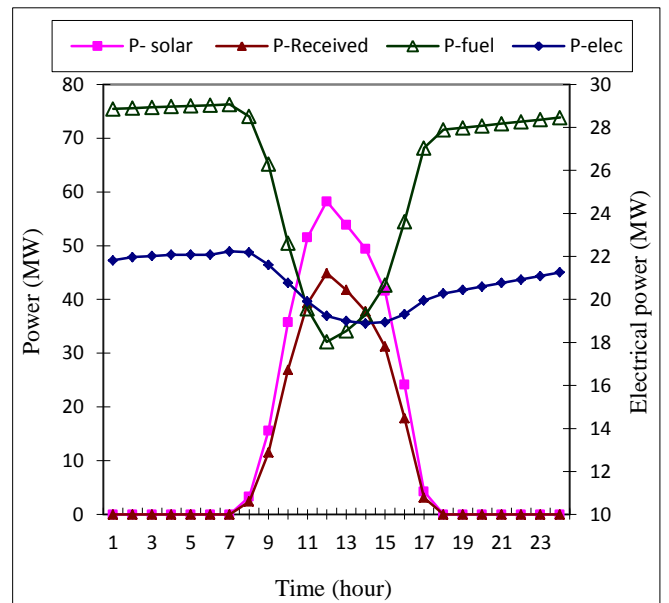


Fig. 14. Temporal evolution of powers in the installation without regeneration (21/12/2006)

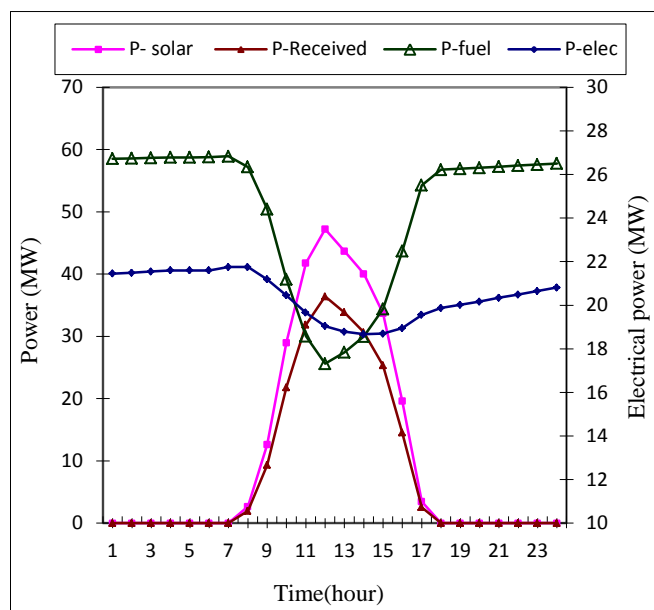


Fig. 15. temporal evolution of powers in the installation with regeneration (21/12/2006)

7. Discussion of Results

The energy analysis results obtained from table 4 and table 6 shows a clear improvement of efficiencies solar-electric and hybrid-electric for the installation with regeneration.

The exergy analysis results in table 5 shows an important loss of exergy efficiency in combustion discharged, results in table 7 prove that we can minimize this loss by introducing a heat regenerator in the solar gas turbine system.

The result in figure 12 and figure 14 shows the impact of ambient temperature in electrical power production and energetic performances of the installation.

When we compare the results of figure 12 with figure 13 and figure 14 with figure 15 we see a reduction in consumption of natural gas (night hours) and a lesser quantity of absorbed solar energy in the installation with regenerator, with keeping an electrical production approximately to the installation without regenerator.

8. Conclusion

In our study, we modelled and simulated a solar gas turbine installation capable to provide an electrical production equal to 20.5 MWe in ISO condition, and then we studied the impact of adding a regenerator in the installation.

The results obtained in this study show a direct impact of the regenerator in improvement of hybrid and solar-electric efficiencies, with a stable production of electrical energy, less consumption of natural gas and reduction heliostats fields' area.

The energy and the exergy balance confirm the impact of the regenerator, by a gain of 4.26 % in exergy efficiency, with high solar-electric efficiency and a cheaper electrical

production due to the reduction of consumption of natural gas and heliostats field's area.

This type of installation is new and very promising especially in regions with duration of sunshine up to 3500 hours/year and a direct normal radiation greater than 2000 kWh/m²/year, such as the south western of Algeria.

References

- [1] S.Bonnet, M. Alaphilippe, P. Stouffs, "Thermodynamic solar energy conversion: Reflections on the optimal solar concentration ratio". *International Journal of Energy, Environment and Economics*, Vol. 12, pp. 141-152, 2006. (Article) .
- [2] Uriyel Fisher, Chemi Sugarmen, Joseph Sinai. "Gas turbine solarization modifications for solar/fuel hybrid operation". *Journal of Turbo machinery* vol.126, pp.872-878, 2004. (Article).
- [3] G. Barigozzi, G. Bonetti, G. Franchini, A. Perdichizzi, S. Ravelli. "Thermal performance prediction of a solar hybrid gas turbine". *Solar Energy* vol.86, pp.2116-2127, 2012. (Article).
- [4] Final publishable report Solgate, solar hybrid gas turbine electric power system (2005). Available: <http://ec.europa.eu/research/energy/pdf/solgate.Reports>.
- [5] Pirre Garcia, Alain Ferrier, G. Flamant, P. Costerg et al. "Solar field efficiency and electricity generation estimations for a hybrid solar gas turbine project in France". *Journal of Solar Energy Engineering* vol.130 pp 0145021-0145023, 2008. (Article).
- [6] Peter Schwarzbozl, Reiner Buck, et al. "Solar gas turbine systems: design, cost and perspective". *Solar Energy* .vol.80, 2006. (Article).
- [7] Peter Heller, Markus Pfänder, et al. "Test and evaluation of a solar powered gas turbine system". *Solar Energy* .vol.80, pp.1225-1230, 2006. (Article).
- [8] Algerian ministry of energy and mining. Available: <http://mem-algeria.org/english/index.php>
- [9] F. Trieb, C. Schillings, M. O'Sullivan, T. Pregger, C. Hoyer-Klick. Global potential of concentrating solar power. German Aerospace Centre (DLR) 2009. (Reports).
- [10] NEAL Algeria. Available: <http://neal-dz.net/activite>.
- [11] Kacem Gairaa, Yahia Bakelli. "An overview of global solar radiation measurements in Ghardaïa area, south Algeria". *International journal of Energy and environment*. Vol.2, pp.255-260, 2011. (Article).
- [12] Climatic condition from METEONORM V 7.0 software.
- [13] Robert Pitz-Paal, Nicolas Bayer Botero, Aldo Steinfeld. "Heliostat field layout optimization for high-temperature solar thermochemical processing". *Solar Energy* vol.85, pp.334-343, 2011. (Article).

- [14] Pierre Garcia, Alain Ferriere, Jean-Jacques Bezian. “Codes for solar flux calculation dedicated to central receiver system applications”. *Solar Energy* vol.82, pp189–197, 2008. (Article).
- [15] Xiudong Wei*, Zhenwu Lu, “A new method for the design of the heliostat field layout for solar tower power plant”. *Renewable Energy* vol.35, pp1970–1975, 2010. (Article).
- [16] Wei XD, Lu ZW, Lin Z. “Optimization procedure for design of heliostat field layout of a 1MWe solar tower thermal power plant”. *Proceedings of the SPIE 2007*. (Conference Paper).
- [17] Abraham Kribus, H. Ries, W. Spirkel. “Inherent limitations of volumetric solar receivers”. *Journal of Solar Energy Engineering* vol.5, pp118-151, 1996. (Article).
- [18] Lukas Feierabend .Thermal model development and simulation of cavity type solar central receiver systems. University of Wisconsin Madison (2009). (Book).
- [19] R.Bernard G.Menguy Schwartz .The solar radiation: thermal conversion and application 2nd edition. (Book).
- [20] John. A. Duffie and William. A. Beckman. Solar engineering of thermal processes, 2nd edition, New York: Wiley (1991). (Book).
- [21] B. Dickey. “Test results from a concentrated solar micro turbine Brayton cycle integration”. *ASME conference proceedings*, pp1031–1036, 2011. (Conference Paper).
- [22] Gregory Nellis, Sanford Klein. Heat transfer. Cambridge University press (2009). (Book).
- [23] TRNSYS STEC 3.0 and TESS available from: <http://sel.me.wisc.edu/trnsys/trnlib/tees/stec.htm>.
- [24] TRNSYS16 Tutorial & application; operation guides. (Book).
- [25] GE Energy, Gas Turbine Performances Data, 2007. (Book).